

# A comparative study of the electronic structures of oxygen- and chlorine-treated nitrogenated carbon nanotubes by x-ray absorption and scanning photoelectron microscopy

S. C. Ray, C. W. Pao, H. M. Tsai, J. W. Chiou,<sup>a)</sup> and W. F. Pong<sup>b)</sup>  
*Department of Physics, Tamkang University, Tamsui 251, Taiwan*

C. W. Chen  
*Department of Material Science and Engineering, National Taiwan University, Taipei 106, Taiwan*

M.-H. Tsai  
*Department of Physics, National Sun Yat-Sen University, Kaohsiung 804, Taiwan*

P. Papakonstantinou  
*NRI, School of Electrical and Mechanical Engineering, University of Ulster at Jordanstown, Newtownabbey, County Antrim, BT370QB Northern Ireland, United Kingdom*

L. C. Chen  
*Center for Condensed Matter Sciences, National Taiwan University, Taipei 106, Taiwan*

K. H. Chen  
*Institute of Atomic and Molecular Sciences, Academia Sinica, Taipei 106, Taiwan*

(Received 24 September 2007; accepted 19 October 2007; published online 13 November 2007)

The electronic structures and bonding properties of oxygen- and chlorine-treated nitrogenated carbon nanotubes (N-CNTs) were studied using x-ray absorption near-edge structure (XANES) and scanning photoelectron microscopy. Features in the C *K*-edge XANES spectra are shifted by  $\sim 0.3$  eV toward higher energies and by  $\sim 1.1$  eV toward lower energies relatively to those of the more symmetrical pyridinlike and graphitelike structured N-CNTs upon chlorination and oxidation, respectively. Increases in N *K*-edge XANES intensities for both chlorination and oxidation reveal substitution of C–C bonds by C–N bonds consistent with the observed valence-band photoemission spectra of the decrease of the C *2s* bond and the increase of the N *2s* bond. © 2007 American Institute of Physics. [DOI: 10.1063/1.2807275]

The chemical modification of carbon nanotubes (CNTs) is of great interest as related changes in their mechanical, electrical, and electronic properties are useful for various applications from nanoelectronic and nanoelectromechanical systems to nanocomposites.<sup>1</sup> Among the numerous chemical modifications/treatments of CNTs; functionalization, dispersion, and chemical doping with various functional groups yield many opportunities for tuning the structural and electronic properties.<sup>2</sup> Ago *et al.*<sup>3</sup> examined various oxidative treatments of CNTs based on the density of states of valence bands and work function. Recently, Watts *et al.*<sup>4</sup> found increases/decreases in the conductivity of CNTs upon oxygen treatment. Weglikowska *et al.*<sup>2</sup> observed a similar increase in the conductivity and change in the Fermi level ( $E_f$ ) during the chemical modification of CNTs. Upon chlorine treatment using dichlorocarbene, the surfaces of CNTs are modified with the presence of other functional forms of carbon.<sup>5</sup> However, upon oxidation and chlorination, not only surface modification but also changes in the structural and electronic properties occur.<sup>2–6</sup> More recently, x-ray absorption results and theoretical calculations have revealed that chlorine-bonded compounds (C–Cl bond) formed on the ni-

trogenated carbon nanotubes (N-CNTs) and their electronic properties changes during the functionalization of N-CNTs in a chlorine plasma atmosphere (N-CNTs:Cl).<sup>7</sup> In the present work, the electronic properties of oxygen-treated N-CNTs (N-CNTs:O) were investigated using C and N *K*-edge x-ray absorption near-edge structure (XANES), scanning photoelectron microscopy (SPEM), and theoretical calculation of the partial density of states (PDOSs); the results are compared with those of N-CNTs:Cl presented elsewhere.<sup>7</sup>

The C and N *K*-edge XANES, SPEM images, and valence-band photoemission spectra were performed at the National Synchrotron Radiation Research Center in Hsinchu, Taiwan. The preparation of the vertically oriented multiwall N-CNTs and N-CNTs:Cl were described elsewhere.<sup>7,8</sup> N-CNTs:O are herein prepared under air-atmospheric plasma conditions using a dielectric barrier discharge system.<sup>9</sup>

Figure 1 displays the normalized C *K*-edge XANES spectra of N-CNTs, N-CNTs:O, N-CNTs:Cl, and highly oriented pyrolytic graphite (HOPG). The  $\pi^*$  features at  $\sim 286.4$ , 285.3, 286.7, and 285.5 eV are associated with  $sp^2$  bonding configuration. The positions of the  $\pi^*$  feature for oxygen/chlorine treated N-CNTs are shifted away from that of untreated N-CNTs because of surface modification and the formation of differently structured N-CNTs. The  $\pi^*$  feature of N-CNTs:O is quite close to that of HOPG and lies below that of N-CNTs by  $\sim 1.1$  eV. The shift of this feature is due to the charge transfer process and the formation of a more graphitelike layered structure.<sup>4,10</sup> Since oxygen/nitrogen has a

<sup>a)</sup>Permanent address: Department of Applied Physics, National University of Kaohsiung, Kaohsiung, Taiwan.

<sup>b)</sup>Author to whom correspondence should be addressed. On leave at Advanced Light Source, Lawrence Berkeley National Laboratory, Berkeley, CA. Electronic mail: wfpong@mail.tku.edu.tw

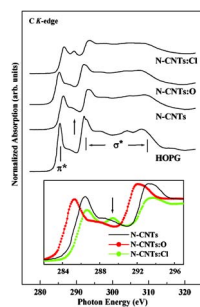


FIG. 1. (Color online) C *K*-edge XANES spectra of N-CNTs, N-CNTs:Cl, and N-CNTs:O and reference HOPG. The inset highlights the  $\pi^*$  region.

greater Pauling electronegativity than carbon [ $O(3.44) > N(3.04) > C(2.55)$ ], the ionic content of the C–N/C–O bond causes electrons to transfer from the tube wall. In the N-CNTs:Cl case, the  $\pi^*$  feature at  $\sim 286.7$  eV is higher than those of HOPG and N-CNTs and has an additional feature at  $\sim 289.2$  eV (indicated by an arrow). These features correspond to the  $1s \rightarrow \pi^*$  transition like that of the pyridine structure with two unfilled  $\pi^*$  orbitals, namely,  $e_{2u}$  (an antibonding state in which wave functions are antisymmetric) and  $b_{2g}$  (a bonding state in which wave functions are symmetric).<sup>10</sup> However, theoretical calculations in the previous work suggested that the feature at  $\sim 289.2$  eV is due to the formation of the C–Cl bond upon chlorination,<sup>7</sup> which was also observed by Unger *et al.*<sup>11</sup> in an x-ray photoelectron spectroscopic (XPS) analysis of Cl-functionalized multiwall CNTs. Chen *et al.* also observed two features at 286.5 and 289.6 eV in the XPS spectrum following the reaction of single-wall CNTs with dichlorocarbene, which are assigned to  $(-\text{CH}_2-\text{C}^*\text{HCl}-)_x$  and  $\text{C}^*\text{HCl}_3$ , respectively.<sup>12</sup> In the  $\sigma^*$  region, the center of the maximum feature in the N-CNTs:O spectrum is located at  $\sim 292.0$  eV, revealing a graphite structure similar to that of HOPG and of N-CNTs:Cl. The feature at  $\sim 293.6$  eV is associated with the pyridine structure.<sup>10</sup> Interestingly, the intensities of  $\pi^*$  (at 286.7 eV) and  $\sigma^*$  (at 293.6 eV) features decrease while that of the additional feature at 289.2 eV, indicated by the arrow, increases for N-CNTs:Cl relative to those for N-CNTs. This trend is not observed for N-CNTs:O, suggesting that N-CNTs:Cl adopts a more symmetric bonding state in the pyridine structure as Cl-bonded compounds. For N-CNTs:O, a very weak shoulder (centered at  $\sim 288$  eV) is observed between  $\pi^*$  and  $\sigma^*$  features similar to HOPG and N-CNTs cases, suggesting the presence of interlayer graphite states similar to the band structure of graphene bilayer<sup>13</sup> or can be the formation of oxygen-bonded carbon atoms. The features in the C *K*-edge XANES spectra of chlorinated and oxidized samples are shifted by  $\sim 0.3$  eV rigidly toward higher energy and by  $\sim 1.1$  eV toward lower energy, respectively, relative to that of untreated N-CNTs, as clearly shown in the inset of Fig. 1, that may also associate with upward and downward band bendings,<sup>14</sup> respectively. To identify these features, the PDOSs of treated (N-CNTs:Cl and N-CNTs:O) and untreated N-CNTs and CNTs are calculated using the CASTEP code,<sup>15</sup> which is a plane-wave pseudopotential method based on the density functional theory and the local density approximation (shown in Fig. 2). The benzene, pyridine, pyridine-Cl, and pyridine-O cluster models represent the local bonding configurations of CNTs, N-CNTs, N-CNTs:Cl, and N-CNTs:O, respectively, whereas hydrogen atoms are used to saturate

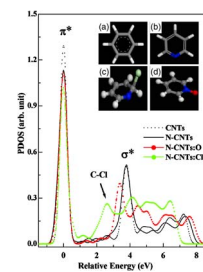


FIG. 2. (Color online) PDOSs of various CNTs. Insets (a)–(d) show cluster models, which represent local bonding configurations of CNTs, N-CNTs, N-CNTs:Cl, and N-CNTs:O respectively. Blue-, green-, and red-colored balls represent N, Cl, and O atoms, respectively.

the dangling bonds of carbon atoms. Insets (a)–(d) in Fig. 2 display the bonding configurations of these four CNTs using blue (N), green (Cl), and red (O) colors which represent the bonding atoms in pure CNTs. Details of the calculations using the cluster models of these CNTs with various geometries can be found elsewhere.<sup>16</sup> In Fig. 2, the first feature in the calculated PDOSs has been aligned with the first feature ( $\pi^*$ ) in the XANES spectra and the unit of intensity has been arbitrarily normalized. The feature at  $\sim 2.6$  eV between  $\pi^*$  and  $\sigma^*$  is obtained from PDOSs of the cluster model of pyridine-Cl with small shift of  $\sigma^*$  at higher energy that corresponds to the C–Cl bond feature observed in C *K*-edge XANES spectra, as indicated by the arrow in the inset of Fig. 1. According to the cluster model of pyridine-O in Fig. 2, the  $\sigma^*$  feature is shifted toward lower energy, as also shown in Fig. 1, due to the formation of more  $sp^2$ -bonded graphitic carbon in the N-CNTs:O observed by Nevidomskyy *et al.*, who found that the  $sp^2$ -bonded carbon feature shifted toward the lower energy in PDOSs calculation of N-CNTs.<sup>17</sup>

Figure 3 displays the N *K*-edge XANES spectra of treated (N-CNTs:Cl and N-CNTs:O) and untreated N-CNTs. The two main features centered at  $\sim 403.2$  and 409.5 eV correspond to the transition to unoccupied  $\pi^*$  and  $\sigma^*$  orbitals, respectively, which are similar to those of the pyridine structure.<sup>10,18</sup> The increase and decrease of the  $\pi^*$  and  $\sigma^*$  intensities, respectively, for both N-CNTs:Cl and N-CNTs:O are due to the substitution of C atoms in N-CNTs by N and O atoms. The difference between the intensities of the  $\pi^*$  and  $\sigma^*$  features in the N *K*-edge XANES spectra of both treated N-CNTs suggests that different atoms were embedded in N-CNTs. The intensity of the  $\sigma^*$  feature at  $\sim 409.5$  eV of N-CNTs:Cl markedly exceeds that of N-CNTs:O, which can be clearly seen in the N *K*-edge spectra difference. This is because chlorination increases the ordering of the crystal

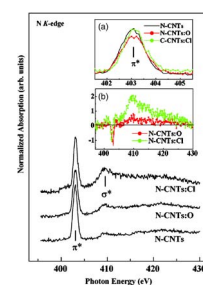


FIG. 3. (Color online) N *K*-edge XANES spectra of N-CNTs, N-CNTs:Cl, and N-CNTs:O. The Inset (a) highlights the  $\pi^*$  region. The Inset (b) shows spectra difference between treated (N-CNTs:Cl and N-CNTs:O) and untreated (N-CNTs).

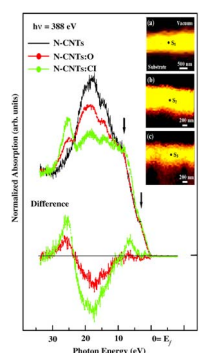


FIG. 4. (Color online) Valence-band photoemission spectra obtained from selected bright spots  $S_1$ ,  $S_2$ , and  $S_3$  of C  $1s$  SPEM cross-sectional images of N-CNTs, N-CNTs:Cl, and N-CNTs:O at an excitation photon energy of 388 eV. The inset shows spectra difference between treated (N-CNTs:Cl and N-CNTs:O) and untreated (N-CNTs).

structure,<sup>19</sup> which can be verified by the formation of the symmetric  $b_{2g}$  bonding state revealed in the C  $K$ -edge XANES spectra.

Figure 4 displays spatially resolved valence-band photoemission spectra of N-CNTs, N-CNTs:Cl, and N-CNTs:O with their corresponding maximum intensity of C  $1s$  SPEM bright cross-sectional images. The spectra in Fig. 4 exhibit photoelectron yields from the bright regions  $S_1$ ,  $S_2$ , and  $S_3$  corresponding to the sidewalls of the respective N-CNTs, N-CNTs:Cl, and CNTs:O. The zero energy refers to  $E_f$ , which is the threshold of the emission spectrum. The spectra reveal two weak structures at binding energies of  $\sim 3.5$  and  $8.2$  eV (marked by downward arrows) associated with the C  $2p$   $\pi$  and  $\sigma$  bonds,<sup>3,7,20,21</sup> respectively. Features centered at  $\sim 15$  eV (mixed  $s$  and  $p$  characters of the C–N bond) and  $18$  eV (C  $2s$ ) are typically observed from nitrogenated carbon films with a graphitic structure.<sup>20</sup> The intensities of these two features ( $15$  and  $18$  eV) decrease for both N-CNTs:Cl and N-CNTs:O relative to the untreated N-CNTs. A new feature in the spectra of both N-CNTs:Cl and N-CNTs:O appears in the range of  $24$ – $30$  eV (centered at  $\sim 25$  eV) and is attributable to N  $2s$  states. This result reflects the increase/decrease in the numbers of C–N/C–C bonds and the formation of nitrogen-based carbon with a pyridine structure, as described by Bhattacharyya *et al.* for  $a$ -CN<sub>x</sub> films.<sup>22</sup> The increase in the intensity of the feature in the range of  $24$ – $30$  eV for both N-CNTs:Cl and N-CNTs:O is also consistent with the increase of  $\sigma^*$  intensity in the N  $K$ -edge XANES spectra. Apparently, the spectra of N-CNTs:Cl reveal increases in the intensity of the  $\sigma$  bond associated with chlorine-derived  $\sigma$  states and can be caused by the formation of C–C and/or C–N–Cl bonds.<sup>7</sup> There is no significant change in the region ( $0$ – $9$  eV) for N-CNTs:O. The spectrum difference between N-CNTs:O/N-CNTs:Cl and N-CNTs shown in the lower inset of Fig. 4 elucidates the effects of oxidation/chlorination. The positive feature centered at  $\sim 25$  eV for N-CNTs:Cl is associated with the formation of chlorine-bonded carbon and/or nitrogen atoms and the presence of a nitrogen lone pair with the enhancement of the N  $2s$  band. The spectrum difference is negative in the region ( $\sim 9$  and  $24$  eV), which indicates a reduction of the C  $2s$ -band states associated with the highly negative intensity at  $\sim 18$  eV.<sup>7,22</sup> For N-CNTs:O the spectrum difference indicates that the intensity difference is essentially 0 in the region,  $0$ – $9$  eV resulted from a small curvature of the graphitic

N-CNTs:O, as observed by Chen *et al.* in multiwall CNTs.<sup>23</sup> The shallow dip at  $17$  eV in the negative spectrum difference of N-CNTs:O is caused by the decrease (increase) in carbon (nitrogen) concentration, while the positive intensity difference at  $26$  eV may be contributed to the N  $2s$  band and/or the O  $2s$  band. Furthermore, the difference in SPEM spectra indicates that the magnitude of the negative (positive) intensity in the range of  $9$ – $24$  eV ( $24$ – $30$  eV) is smaller (larger) for N-CNTs:Cl than for N-CNTs:O, suggesting that the number of C–C bonds that were substituted by C–N bonds and the formation of N  $2s$  bonds were more for N-CNTs:Cl. The reduction ( $9$ – $24$  eV)/enhancement ( $24$ – $30$  eV) of feature intensity between treated and untreated N-CNTs may be due to the greater delocalization of C  $2p$   $\pi$  electrons by coupling with neighboring N-CNTs, as observed by Choi *et al.*<sup>24</sup> for double-walled CNTs and the related formation of oxygen/chlorine-bonded carbon and/or nitrogen atoms, which change the electronic/bonding structures.

<sup>1</sup>M. S. Dresselhaus, G. Dresselhaus, and P. Avouris, *In Carbon Nanotubes: Synthesis, Structure, Properties and Applications*, Topic in Applied Physics Vol. 80 (Springer, New York, 2001).

<sup>2</sup>U. D. Weglikowska, V. Skákalová, R. Graupner, S. H. Jhang, B. H. Kim, H. J. Lee, L. Ley, Y. W. Park, S. Berber, D. Tománek, and S. Roth, *J. Am. Chem. Soc.* **127**, 5125 (2005).

<sup>3</sup>H. Ago, T. Kugler, F. Cacialli, W. R. Salaneck, M. S. P. Shaffer, A. H. Windle, and R. H. Friend, *J. Phys. Chem. B* **103**, 8116 (1999).

<sup>4</sup>P. C. P. Watts, N. Mureau, Z. Tang, Y. Miyajima, J. D. Carey, and S. R. P. Silva, *Nanotechnology* **18**, 175701 (2007).

<sup>5</sup>W. H. Lee, S. J. Kim, W. J. Lee, J. G. Lee, R. C. Haddon, and P. J. Reucroft, *Appl. Surf. Sci.* **181**, 121 (2001).

<sup>6</sup>S. S. Roy, P. Papakonstantinou, T. I. T. Okpalugo, and M. Murphy, *J. Appl. Phys.* **100**, 053703 (2006).

<sup>7</sup>S. C. Ray, C. W. Pao, H. M. Tsai, J. W. Chiou, W. F. Pong, C.-W. Chen, M.-H. Tsai, P. Papakonstantinou, L. C. Chen, K. H. Chen, and W. G. Graham, *Appl. Phys. Lett.* **90**, 192107 (2007).

<sup>8</sup>L. C. Chen, C. Y. Wen, C. H. Liang, W. K. Hong, K. J. Chen, H. C. Cheng, C. S. Shen, C. T. Wu, and K. H. Chen, *Adv. Funct. Mater.* **12**, 687 (2002).

<sup>9</sup>T. I. T. Okpalugo, P. Papakonstantinou, H. Murphy, J. McLaughlin, and N. M. D. Brown, *Carbon* **43**, 2951 (2005).

<sup>10</sup>S. Bhattacharyya, M. Lübke, and F. Richter, *J. Appl. Phys.* **88**, 5043 (2000).

<sup>11</sup>E. Unger, A. Graham, F. Kreupl, M. Liebau, and W. Hoenlein, *Curr. Appl. Phys.* **2**, 107 (2002).

<sup>12</sup>Y. Chen, R. C. Haddon, S. Fang, A. M. Rao, P. C. Eklund, W. H. Lee, E. C. Dickey, E. A. Grulke, J. C. Pendergrass, A. Chavan, B. E. Haley, and R. E. Smalley, *J. Mater. Res.* **13**, 2423 (1998).

<sup>13</sup>D. A. Fischer, R. M. Wentzcovitch, R. G. Carr, A. Continenza, and A. J. Freeman, *Phys. Rev. B* **44**, 1427 (1991).

<sup>14</sup>S. H. Lim, H. I. Elim, X. Y. Gao, A. T. S. Wee, W. Ji, J. Y. Lee, and J. Lin, *Phys. Rev. B* **73**, 045402 (2006).

<sup>15</sup>M. C. Pyane, M. Teter, D. C. Allan, and J. D. Joannopoulos, *Rev. Mod. Phys.* **64**, 1045 (1992).

<sup>16</sup>C.-W. Chen and M.-H. Lee, *Nanotechnology* **15**, 480 (2004).

<sup>17</sup>A. H. Nevidomskyy, G. Csányi, and M. C. Payne, *Phys. Rev. Lett.* **91**, 105502 (2003).

<sup>18</sup>I. Jiménez, W. M. Tong, D. K. Shuh, B. C. Holloway, M. A. Kelly, P. Pianetta, L. J. Terminello, and F. J. Himpsel, *Appl. Phys. Lett.* **74**, 2620 (1999).

<sup>19</sup>I. Shimoyama, G. Wu, T. Sekiguchi, and Y. Baba, *Phys. Rev. B* **62**, R6053 (2000).

<sup>20</sup>S. Suzuki, Y. Watanabe, T. Kiyokura, K. G. Nath, T. Ogino, S. Heun, W. Zhu, C. Bower, and O. Zhou, *Phys. Rev. B* **63**, 245418 (2001).

<sup>21</sup>J. W. Chiou, C. L. Yueh, J. C. Jan, H. M. Tsai, W. F. Pong, I. H. Hong, R. Klausner, M.-H. Tsai, Y. K. Chang, Y. Y. Chen, C. T. Wu, K. H. Chen, S. L. Wei, C. Y. Wen, L. C. Chen, and T. J. Chuang, *Appl. Phys. Lett.* **81**, 4189 (2002).

<sup>22</sup>S. Bhattacharyya, C. Spaeth, and F. Richter, *J. Appl. Phys.* **89**, 2414 (2001).

<sup>23</sup>P. Chen, X. Wu, X. Sun, J. Lin, W. Ji, and K. L. Tan, *Phys. Rev. Lett.* **82**, 2548 (1999).

<sup>24</sup>H. C. Choi, S. Y. Kim, W. S. Jang, S. Y. Bae, J. Park, K. L. Kim, and K. Kim, *Chem. Phys. Lett.* **399**, 255 (2004).